Electronic Supplementary Material (ESI) for Chemical Communications.

Lead Encapsulation by a Gold-clamp through Electrostatic, Metallophilic, Hydrogen Bonding and Weak Interactions.

Raquel Echeverría, José M. López-de-Luzuriaga,* Miguel Monge, Sonia Moreno, M. Elena Olmos and María Rodríguez-Castillo

ELECTRONIC SUPPLEMENTARY INFORMATION

Experimental Section.

General. All reactions were carried out under dry and deoxygenated argon atmosphere. All solvents were distilled. [Au(*o*-C_6BrF_4)(tht)] and [Pb{$HBpz_3$}Cl] were prepared according to literature methods.[1,2]

Materials and Physical Measurements. Infrared spectra were recorded in the 4000-450 cm^{-1} range on a Perkin-Elmer FT-IR Spectrum Two with an ATR (Single Reflection Diamond) accessory. ^1H and ^{19}F NMR spectra were recorded on a Bruker Avance 400 in chloroform solutions. Chemical shifts are quoted relative to $SiMe_4$ (^1H external) and $CFCl_3$ (^{19}F external). C, H, N analyses were carried out with a C.E. Instrument EA-1110 CHNS-O microanalyzer. The MALDI mass spectra were registered on a Microflex Bruker spectrometer using DIT (Dithranol) and DCTB (T-2-(3-(4-t-butylphenyl)-2-methyl-2-propenylidene)-malononitrile) as the matrix. The m/z values are given for the higher peak in the isotopic pattern.

Synthesis of [NBu_4][Au_3(*o*-C_6BrF_4)$_3$($HBpz_3$)] (1). To a solution of [Au(*o*-C_6BrF_4)(tht)] (0.305 g, 0.6 mmol) in dichloromethane (30 mL) was added K[$HBpz_3$] (0.05 g, 0.2 mmol) and [NBu_4]Br (0.064 g, 0.2 mmol). The reaction mixture was stirred for 3 h at 0º C and filtered off. Evaporation of the solvent under vacuum, and addition of *n*-hexane gave rise to complex **1** as a white solid. Yield 60% (0.2057 g). ^1H NMR (300 MHz, $CDCl_3$, 298 K), δ 7.77 (s, 1H, H_5), 7.46 (s, 1H, H_3), 6.38 (s, 1H, H_4) ppm. ^{19}F NMR (282 MHz, $CDCl_3$, 298 K) δ −113.90 (dd, 1F, F_1), −127.15 (dd, 1F, F_4), −157.89 (dd, 1F, F_2), −159.49 (pt, 1F, F_3) ppm. FT-IR (ATR): ν = 825, 1008, 1596 y 1615 cm^{-1} (Au-*o*-C_6BrF_4), ν = 2476 cm^{-1} (B−H), ν = 1482 cm^{-1} (B-N). MALDI(+): m/z (%): 242 (100) $[NBu_4]^+$; MALDI(−): m/z (%): 1488 (100) [Au_3(*o*-C_6BrF_4)$_3$($HBpz_3$)]$^-$; elemental analysis calcd. (%) for $C_{43}H_{46}Au_3BBr_3F_{12}N_7$: C, 29.85; H, 2.68; N, 5.67. Found: C, 29.93; H, 2.74; N, 5.59. Λ_M (acetonitrile): 105 Ω^{-1} cm^2 mol^{-1}.

Synthesis of [{Pb($HBpz_3$)}{Au_3(*o*-C_6BrF_4)$_3$($HBpz_3$)}] (2). To a solution of the complex **1** (0.346 g, 0.2 mmol) in diethyl ether (30 mL) was added [Pb{$HBpz_3$}Cl] (0.09 g, 0.2 mmol), and a white precipitate (NBu_4Cl) was immediately formed. The reaction mixture was stirred for 2 h at 0º C and filtered off. Evaporation of the solvent under vacuum, and addition of *n*-hexane gave rise to complex **2** as a white solid. Yield 45% (0.1531 g). ^1H NMR (400 MHz, $CDCl_3$, 298 K), δ 7.95, 7.78, 7.65, 7.19, 6.55, 6.23 ppm. ^{19}F NMR (376 MHz, $CDCl_3$, ppm) δ −112.90 (dd, 1F, F_1), −126.33 (dd, 1F, F_4), −156.38 (dd, 1F, F_2), −157.54 (pt, 1F, F_3). FT-IR (ATR): ν = 1051 y 1486 cm^{-1} (Au-*o*-C_6BrF_4), ν = 2454 y 2489 cm^{-1} (B−H), ν = 1482 y 1506 cm^{-1} (B-N). MALDI(+): m/z

(%): 421 (100) $[Pb(HBpz_3)]^+$; MALDI(−): m/z (%): 1488 (100) $[Au_3(o\text{-}C_6BrF_4)_3(HBpz_3)]^-$; elemental analysis calcd. (%) for $C_{36}H_{20}Au_3B_2Br_3F_{12}N_{12}Pb$: C, 22.66; H, 1.06; N, 8.81. Found: C, 22.54; H, 1.11; N, 9.01. Λ_M (acetonitrile): 72 Ω^{-1} cm^2 mol^{-1}.

Crystallography.

The single crystal X-ray diffraction data for **1** were collected in ω and ϕ scan mode with a Nonius Kappa CCD diffractometer, using Mo Kα X-rays obtained from a graphite monochromator. A colorless needle [0.18 mm x 0.05 x 0.025 mm], obtained by slow slow diffusion of *n*-hexane into a solution of the complex in diethyl ether, was attached to a glass fiber and transferred to the cold gas stream (198K) of an Oxford Instruments low-temperature attachment at. Data were collected up to 2Θ of 54° (resolution 0.78) with ω and ϕ scans. Absorption correction was based on multiple scans.[3] The structure was solved by using Patterson[4] and refined on F_o^2 with SHELXL.[5] All nonhydrogen atoms were treated anisotropically, and all hydrogen atoms were included as riding bodies.

The single crystal X-ray diffraction data for **2** were collected in ω and ϕ scan mode with a Nonius Kappa CCD diffractometer, using Mo Kα X-rays obtained from a graphite monochromator. A colorless plate [0.1 mm x 0.1 x 0.05 mm], obtained by slow slow diffusion of *n*-hexane into a solution of the complex in diethyl ether, was attached to a glass fiber and transferred to the cold gas stream (193K) of an Oxford Instruments low-temperature attachment at. Data were collected up to 2Θ of 56° (resolution 0.75) with ω and ϕ scans. Absorption correction was based on multiple scans.[3] The structure was solved by using direct methods[6] and refined on F_o^2 with SHELXL.[5] All nonhydrogen atoms were treated anisotropically, and all hydrogen atoms were included as riding bodies.

CCDC 1582222−1582223 contain the supplementary crystallographic data for this paper. These data can be obtained free of charge via www.ccdc.cam.ac.uk/ data_request/cif, or by emailing data_request@ccdc.cam.ac.uk, or by contacting The Cambridge Crystallographic Data Centre, 12 Union Road, Cambridge CB2 1EZ, UK; fax: +44 1223 336033.

Computational details.

All calculations were performed using the TURBOMOLE v6.4[7] and the Gaussian 09 suite of programs[8] using DFT/PBE,[9] Hartree-Fock and MP2[10] levels of theory.

In a first step we have optimized model **2a** at DFT-D3/PBE level, including the empirical dispersion correction by Grimme et al.[11] This level of theory has been proven to represent non-covalent interactions at lower computational cost. We have also optimized model 2a at HF level of theory. For these calculations the corresponding def2-TZVP basis sets were used.[12] The DFT-optimized model has been employed as starting point to deepen in the study of the intrinsic nature of the interaction between fragments $\{Pb(HBpz_3)\}^+$ and $\{Au_3(o\text{-}C_6BrF_4)_3(HBpz_3)\}^-$. For this, we have calculated the BSSE-corrected interaction energies at the DFT-D3 optimised distance both at HF and MP2 levels of theory using the SDD basis sets with Stuttgart/Dresden quasirelativistic (QR) ECPs for Z>2,[13] as implemented in Gaussian09. The HF level represent the ionic component of the interaction between fragments, whereas the MP2 level includes both the ionic and the dispersive components, what permits to account for both contributions to the interaction between the trinuclear Au(I) host.

The interaction energy between ionic counterparts at Hartree-Fock (HF) and MP2 levels of theory was obtained according to equation:

$$\Delta E = E_{AB}^{(AB)} - E_{A}^{(AB)} - E_{B}^{(AB)} = V(R)$$

A counterpoise correction for the basis-set superposition error (BSSE)[14] on ΔE (or E_{int}) was thereby performed. We fitted the calculated points using a four-parameter equation, which had been previously used[15] to derive the Herschbach-Laurie relation:[16]

$$\Delta E = V(R) = Ae^{-BR} - CR^{-n}$$

The binding energy between the host Au(I) and the guest Pb(II) fragments (E_{bind}) was computed considering the relaxation of the separate counterparts and, therefore, considering the deformation energy (E_{def}) required to change the host and guest units from the corresponding minium-energy geometries to the geometry acquired in the assembly:

$$E_{bind} = E_{def} + E_{int}$$

where

$$E_{def} = (E^{AB}{}_{A} - E^{A}{}_{A}) + (E^{AB}{}_{B} - E^{B}{}_{B})$$

$E^{X}{}_{Y}$ is the energy of fragment Y at the geometry of X. AB is the host-guest system; A is the host and B is the guest.

As we have mentioned in the introduction one of the most important factors affecting the heavy metals behavior are the relativistic effects. We have also studied the influence of relativistic effects on the Au(I) and Pb(II) metal centres by using non-relativistic (NR) effective core potentials (ECPs) for both metal centers.

We have also checked the NBO charges at MP2 level in order to explain the ionic contribution to the interaction between $\{Pb(HBpz_3)\}^+$ and $\{Au_3(o\text{-}C_6BrF_4)_3(HBpz_3)\}^-$ fragments. For a better representation of the interaction between charges we computed the Electrostatic Potential (ESP) of the MP2 density (isovalue 0.004) for model system $[\{Pb(HBpz_3)\}\{Au_3(o\text{-}C_6BrF_4)_3(HBpz_3)\}]$ (**2a**).

The NCI data representing the reduced density gradient versus the electron density multiplied by the sign of the second Hessian eigenvalue (λ_2) as well as the cube files representing the gradient isosurface that displays the non-covalent interactions in the real space were computed with NCIplot.[17]

References.

[1] R. Usón, A. Laguna, J. Vicente, J. García, *Organomet. Chem.*, 1977, **131**, 471-475.

[2] D. L. Reger, M. F. Huff, A. L. Rheingold, B. S. Haggertyt, *J. Am. Chem. Soc.* 1992, **114**, 579-584.

[3] R. H. Blessing, *Acta Cryst. A* **1995**, *51*, 33.

[4] A. L. Patterson, *Phys. Rev.* **1934**, *46*, 372.

[5] G. M. Sheldrick, SHELXL-97; University of Göttingen: Göttingen, Germany, 1997.

[6] (a) Sheldrick, G. M. *Acta Crystallogr. A* **2008**, *64*, 112. (b) Altomare, A.; Cascarano, G.; Giacovazzo, C.; Guagliardi, A.; Burla, M. C.; Polidori, G.; Camalli, M. *J. Appl. Crystallogr*. **1994**, *27*, 435.

[7] TURBOMOLE V6.4 2012, a development of University of Karlsruhe and Forschungszentrum Karlsruhe GmbH, 1989-2007, TURBOMOLE GmbH, since 2007; available from http://www.turbomole.com.

[8] Gaussian 09, Revision A.1, Frisch, M. J.; Trucks, G. W.; Schlegel, H. B.; Scuseria, G. E.; Robb, M. A.; Cheeseman, J. R.; Scalmani, G.; Barone, V.; Mennucci, B.; Petersson, G. A.; Nakatsuji, H.; Caricato, M.; Li, X.; Hratchian, H. P.; Izmaylov, A. F.; Bloino, J.; Zheng, G.; Sonnenberg, J. L.; Hada, M.; Ehara, M.; Toyota, K.; Fukuda, R.; Hasegawa, J.; Ishida, M.; Nakajima, T.; Honda, Y.; Kitao, O.; Nakai, H.; Vreven, T.; Montgomery, Jr., J. A.; Peralta, J. E.; Ogliaro, F.; Bearpark, M.; Heyd, J. J.; Brothers, E.; Kudin, K. N.; Staroverov, V. N.; Kobayashi, R.; Normand, J.;

Raghavachari, K.; Rendell, A.; Burant, J. C.; Iyengar, S. S.; Tomasi, J.; Cossi, M.; Rega, N.; Millam, N. J.; Klene, M.; Knox, J. E.; Cross, J. B.; Bakken, V.; Adamo, C.; Jaramillo, J.; Gomperts, R.; Stratmann, R. E.; Yazyev, O.; Austin, A. J.; Cammi, R.; Pomelli, C.; Ochterski, J. W.; Martin, R. L.; Morokuma, K.; Zakrzewski, V. G.; Voth, G. A.; Salvador, P.; Dannenberg, J. J.; Dapprich, S.; Daniels, A. D.; Farkas, Ö.; Foresman, J. B.; Ortiz, J. V.; Cioslowski, J.; Fox, D. J. Gaussian, Inc., Wallingford CT, **2009**.

[9] a) Parr, R. G.; Yang, W. *Density-functional theory of atoms and molecules*; Oxford University Press: New York, 1989. b) Lee, C.; Yang, W.; Parr, R. G. *Phys. Rev. B* 1988, **37**, 785.

[10] a) Møller, C.; Plesset, M.S. *Phys.Rev.* 1934, **46**, 618. b) Hehre, W.J.; Radom, L.; Schleyer, P.v.R.; Pople, J.A. *Ab Initio Molecular Orbital Theory*; John Wiley: New York, 1986.

[11] S. Grimme, J. Antony, S. Ehrlich, H. Krieg, *J. Chem. Phys.* 2010, **132**, 154104.

[12] F. Weigend, R. Ahlrichs, *Phys. Chem. Chem. Phys.* 2005, **7**, 3297.

[13] a) T. H. Dunning Jr. and P. J. Hay, in *Modern Theoretical Chemistry*, Ed. H. F. Schaefer III, Vol. 3 (Plenum, New York, 1977) 1-28; b) D. Andrae, U. Haeussermann, M. Dolg, H. Stoll, H. Preuss, *Theor. Chim. Acta,* 1990, **77**, 123; c) B. Metz, H. Stoll, M. Dolg, *J. Chem. Phys.*, 2000, **113**, 2563.

[14] S. F. Boys, F. Bernardi, *Mol. Phys.,* 1970, **19**, 553.

[15] P. Pyykkö, *Chem. Rev.*, 1997, **97**, 597.

[16] D. R. Herschbach, V. W. Laurie, *J. Chem. Phys.,* 1961, **35**, 458.

[17] J. Contreras-García, E. R. Johnson, S. Keinan, R. Chaudret, J.-P. Piquemal, D. N. Beratan, W. Yang, *J. Chem. Theory Comput.* 2011, **7**, 625.

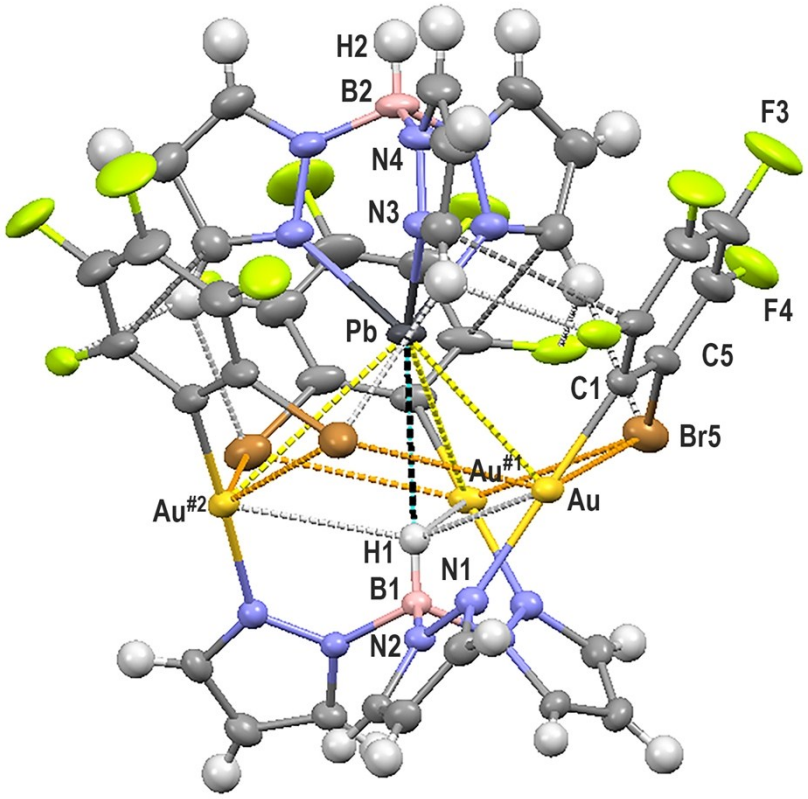

Figure S1. Crystal structure of **2** with the labelling scheme for the atom positions showing the different types of weak interactions.

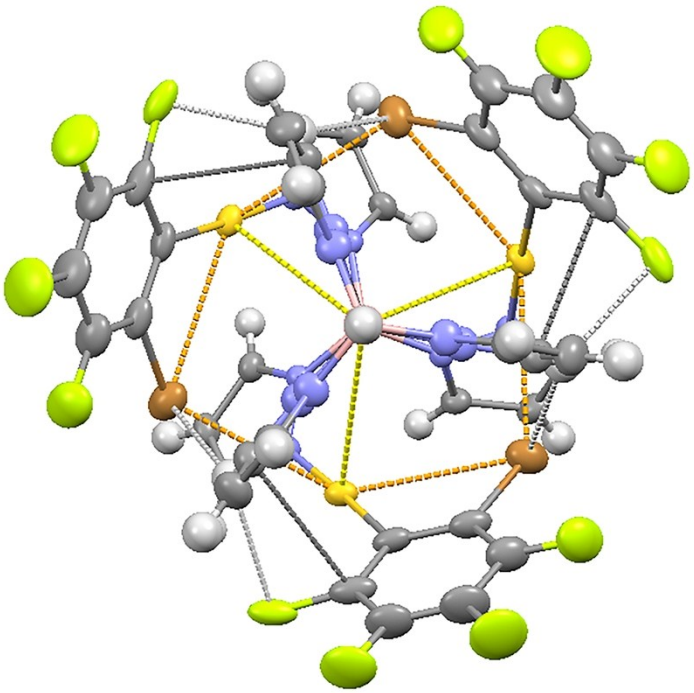

Figure S2. Crystal structure of **2** viewed from the crystallographic *b* axis. Color code: gold: yellow; lead: black; nitrogen: blue; boron: pink; carbon: grey; fluorine: green; bromine: brown; hydrogen: light grey.

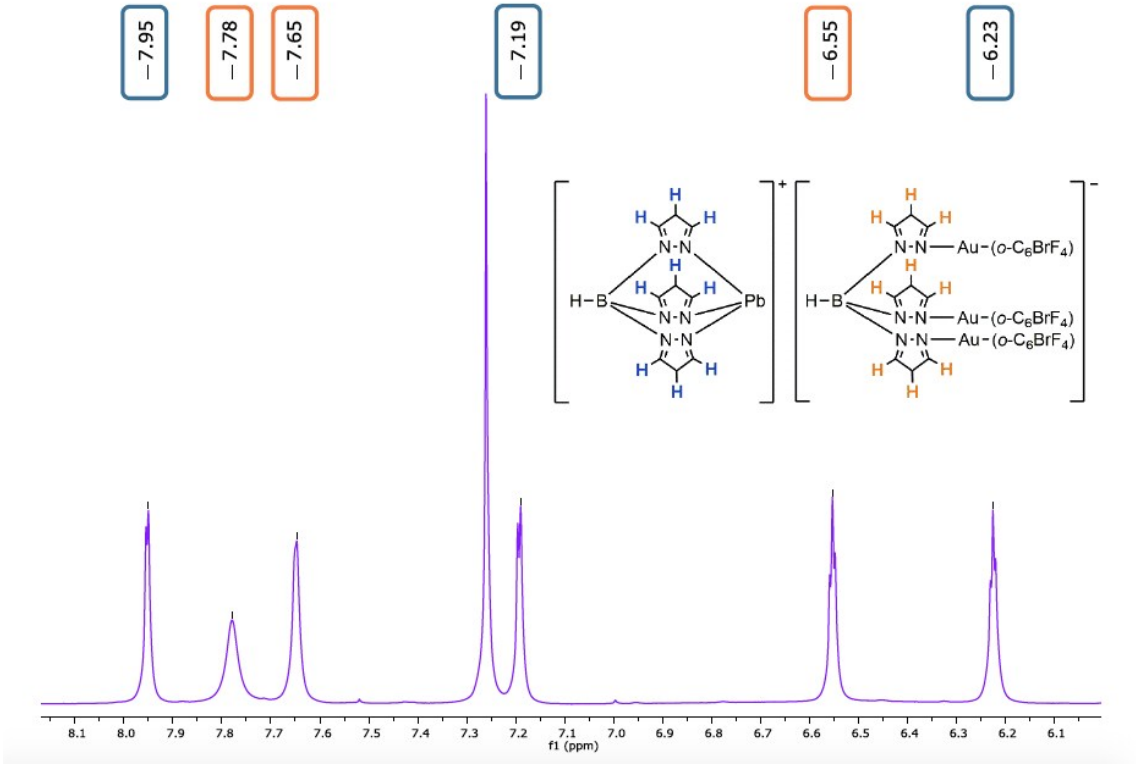

Figure S3. ^{1}H NMR spectrum of complex **2** in $CDCl_3$.

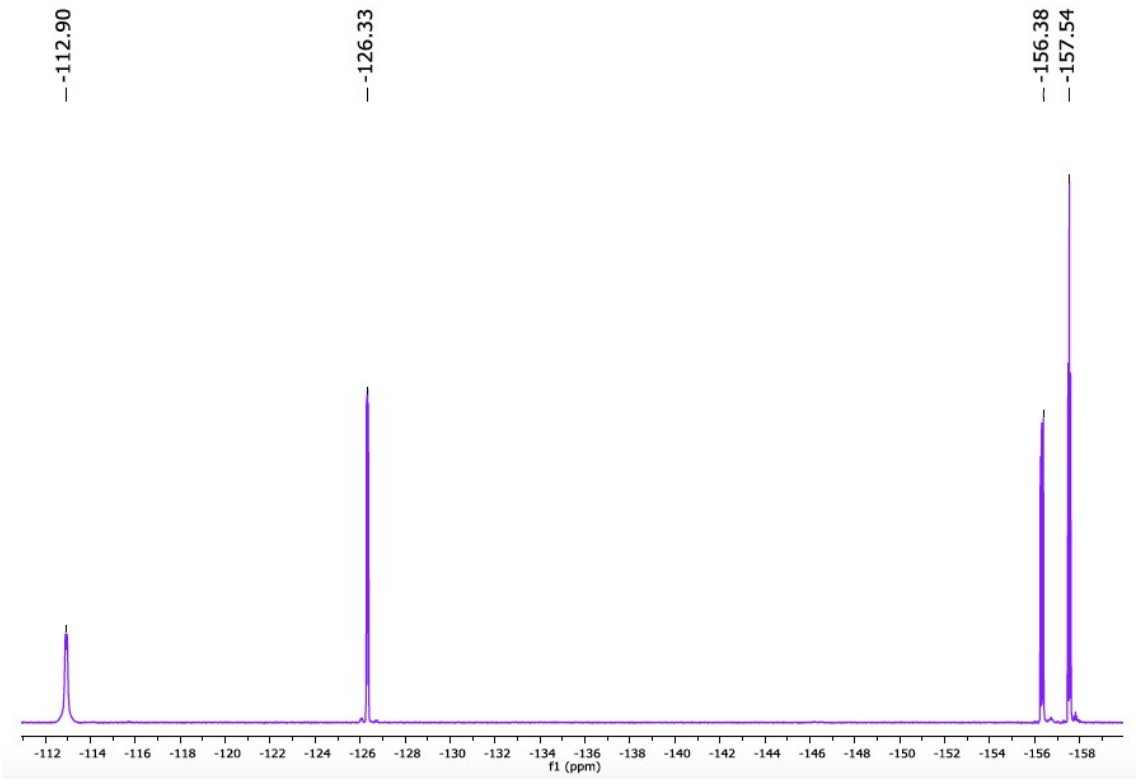

Figure S4. ^{19}F NMR spectrum of complex **2** in $CDCl_3$.

Table S1. Selected experimental structural parameters for complex **2** and optimized parameters for model system **2a** at the equilibrium distances obtained at HF and DFT-D3 levels of theory (distance in Å and angles in deg).

	Au-C	Au-N	Pb-N	B-H	C-Au-N	N-Pb-N	Au···H[a]	Au···Pb	Au···Au	Pb···H[b]	Au···Br[c]	C···C[d]	H···F[e]	H···Br[e]	Pb···Br
Exp	2.006	2.064	2.365	0.980	178.4	79.06	3.019	3.857	5.116	3.102	3.405 3.518	3.251	2.593	2.897	4.001
HF	2.075	2.138	2.372	1.196	176.0	79.0	3.083	4.261	5.254	3.541	3.587 4.488	3.657	2.636	3.252	4.879
DFT-D3	2.011	2.081	2.434	1.211	177.9	77.4	2.933	3.774	5.008	2.919	3.499 3.674	3.154	2.369	2.794	4.225

[a] Interaction between Au and H-B bond; [b] interaction between Pb and H-B bond;[c] interactions between the Br atom of a C_6BrF_4 ligand with two adjacent Au centres; [d] interactions between C atoms from pyrazolate ligands bonded to Pb(II) and C_6F_4Br ligands; [e] interactions between a H atom of a pyrazolate ligand bonded to Pb(II) and F or Br atoms of adjacent C_6BrF_4 ligands.

XYZ COORDINATES OF THE DFT OPTIMISED MODEL SYSTEMS

Model **1a** (complex **1**) optimised at DFT-D3 level of theory

C	-1.18278	-0.20135	-6.22901
C	-0.06760	0.20069	-5.48646
C	-2.26414	-0.08403	-5.33419
C	2.63853	1.63276	-4.10049
C	3.93693	1.12110	-4.05075
C	-0.57835	3.44209	-3.59591
C	3.85258	0.03594	-3.15319
C	-0.63900	4.66816	-2.92720
C	-0.05542	4.41337	-1.66999
C	-3.79086	0.84534	-0.58812
C	-4.87503	0.05509	-0.15127
C	-3.28325	1.76165	0.34872
C	-5.41454	0.16074	1.14082
C	1.40866	-2.36129	0.49691
C	2.39280	-3.02977	1.23988
C	0.09383	-2.42418	1.01512
C	-3.78784	1.88678	1.65217
C	-4.86552	1.08083	2.04753
C	3.37121	0.69175	1.58348
C	2.00509	1.03736	1.50428
C	-0.21091	-3.11142	2.20163
C	2.12228	-3.72675	2.42864
C	3.87688	-0.18766	2.55348
C	1.17224	0.47103	2.48360
C	0.80697	-3.76957	2.91043
C	3.00322	-0.74467	3.49952
C	1.64306	-0.40656	3.47151
H	-1.20278	-0.54457	-7.26072
H	0.98611	0.25659	-5.75258
H	-3.32212	-0.30264	-5.47081
H	2.22454	2.48703	-4.63487
H	4.81825	1.49196	-4.56912
H	-0.93245	3.14550	-4.58167
H	4.62621	-0.63436	-2.78273
H	-1.06332	5.60138	-3.29022
H	0.04206	0.38584	-2.02590
H	0.09446	5.07088	-0.81540
Au	-2.85768	0.63407	-2.35504
Au	1.93680	-1.27651	-1.11138
Au	1.18751	2.08687	-0.00349
B	0.33254	1.03219	-3.00258
Br	-5.67332	-1.23994	-1.29988
Br	4.63202	1.37765	0.32774
Br	-1.34513	-1.53662	0.14440
F	-2.24899	2.56466	0.02328
F	-6.45117	-0.59211	1.54325
F	3.68838	-3.00290	0.84677

F	-3.26747	2.76750	2.51700
F	-5.37540	1.19734	3.28304
F	5.17513	-0.52476	2.60442
F	3.10182	-4.34692	3.10565
F	-1.45930	-3.16470	2.69138
F	-0.15088	0.73199	2.49228
F	0.52494	-4.43092	4.04437
F	3.46378	-1.60544	4.42085
F	0.80714	-0.95150	4.37021
N	-0.48037	0.53429	-4.23566
N	-1.82175	0.35598	-4.13870
N	1.84644	0.88005	-3.28911
N	2.59040	-0.09198	-2.70273
N	0.00700	2.53361	-2.77156
N	0.32570	3.12371	-1.59483

Model **2a** (complex **2**) optimised at DFT-D3 level of theory

C	0.14382	-2.89702	-2.21091
C	1.07088	-3.91162	-1.92338
C	2.29045	-4.05549	-2.60304
C	2.59826	-3.17293	-3.65044
C	1.67508	-2.17753	-4.01086
C	0.47661	-2.05001	-3.29097
C	-3.86918	-3.52124	0.73822
H	-3.58788	-4.55814	0.55956
C	-4.87569	-2.98031	1.56094
H	-5.57961	-3.51568	2.19328
C	-4.75530	-1.59771	1.40123
H	-5.31065	-0.77534	1.84813
Au	-1.50467	-2.68166	-1.07970
B	-3.20767	0.00118	0.00037
H	-1.99637	0.00073	0.00023
Br	-0.72245	-0.67030	-3.83339
F	0.81807	-4.80133	-0.93727
F	3.16064	-5.01276	-2.26157
F	3.75194	-3.29294	-4.31508
F	1.97717	-1.36428	-5.03127
N	-3.19178	-2.52534	0.12897
N	-3.73681	-1.35229	0.53416
C	-3.86679	2.40168	2.68224
H	-3.58485	2.76528	3.66934
C	-4.87353	2.84416	1.80290
H	-5.57701	3.65976	1.95079
C	-4.75406	2.01452	0.68536
H	-5.30987	1.99057	-0.25005
N	-3.19013	1.37577	2.12406
N	-3.73585	1.14034	0.90586
C	-3.86794	1.12382	-3.41914

H	-3.58609	1.79677	-4.22781
C	-4.87510	0.14142	-3.36222
H	-5.57909	-0.13794	-4.14216
C	-4.75526	-0.41154	-2.08505
H	-5.31119	-1.20949	-1.59631
N	-3.19070	1.15299	-2.25198
N	-3.73645	0.21592	-1.43870
C	0.14536	-0.46632	3.61427
C	1.07312	0.28956	4.34872
C	2.29269	-0.22761	4.81261
C	2.59977	-1.57609	4.57178
C	1.67589	-2.38549	3.89044
C	0.47745	-1.82524	3.42065
Au	-1.50310	0.40646	2.86294
Br	-0.72258	-2.98433	2.49755
F	0.82103	1.58856	4.62626
F	3.16354	0.54632	5.47038
F	3.75343	-2.09212	5.00751
F	1.97730	-3.67598	3.69608
C	0.14620	3.36311	-1.40342
C	1.07358	3.62081	-2.42573
C	2.29355	4.28060	-2.21031
C	2.60146	4.74609	-0.92224
C	1.67801	4.56119	0.11987
C	0.47913	3.87474	-0.12982
Au	-1.50294	2.27685	-1.78270
Br	-0.72028	3.65547	1.33603
F	0.82069	3.21188	-3.68925
F	3.16400	4.46289	-3.20989
F	3.75552	5.38094	-0.69367
F	1.98022	5.03805	1.33441
C	2.49011	-3.00904	0.74520
H	1.51056	-3.45991	0.88786
C	3.76580	-3.59875	0.81105
H	4.00315	-4.63812	1.02224
C	4.65206	-2.55128	0.54630
H	5.73916	-2.52701	0.49281
B	4.44743	-0.00162	-0.00049
H	5.65843	-0.00207	-0.00063
N	3.93075	-1.41997	0.33672
N	2.60606	-1.69748	0.45751
Pb	0.92223	-0.00033	-0.00010
C	2.49217	2.14876	2.23211
H	1.51293	2.49813	2.55171
C	3.76825	2.50008	2.70934
H	4.00629	3.20254	3.50370
C	4.65379	1.74660	1.93409
H	5.74087	1.68769	1.93929
N	3.93171	0.99974	1.05945
N	2.60722	1.24380	1.24000
C	2.49111	0.85756	-2.97812

H	1.51170	0.96009	-3.43996
C	3.76703	1.09455	-3.52163
H	4.00474	1.43120	-4.52727
C	4.65294	0.79958	-2.48193
H	5.74006	0.83302	-2.43400
N	3.93122	0.41592	-1.39747
N	2.60660	0.45087	-1.69845